

## EMMA INJECTION AND EXTRACTION\*

B. D. Muratori<sup>#</sup>, J. K. Jones, STFC Daresbury Laboratory, Y. Giboudot, Brunel University, D. J. Holder, University of Liverpool, and Cockcroft Institute, UK

### Abstract

EMMA (Electron Machine with Many Applications) is a prototype non-scaling electron FFAG hosted at Daresbury Laboratory [1,2]. NS-FFAGs related to EMMA have an unprecedented potential for medical accelerators for carbon and proton hadron therapy. They could also be used as the accelerator for a sub-critical reactor. We summarise the design and commissioning of both the injection and extraction lines for this machine.

### INTRODUCTION

Non-scaling Fixed-Field Alternating Gradient (ns-FFAG) accelerators were first conceived to provide very rapid acceleration for muon beams and have since been further developed for a wide range of potential applications. These range from the next generation of high-energy proton and heavy-ion accelerators; accurate and cost-effective particle beam cancer therapy machines (such as PAMELA [3]); to the accelerator component of Accelerator-Driven Subcritical (nuclear) Reactors (ADSR). EMMA, currently being commissioned at Daresbury Laboratory, in the UK, is an electron-model of an ns-FFAG designed and built to demonstrate the operation of such machines. Successful commissioning and operation of EMMA is a world's first for this new concept in accelerator design.

For their application in ADSRs, fission is enabled by high-energy proton beams spallating neutrons from a target embedded in a thorium-fuelled reactor [4]. NS-FFAGs have also been adopted as the baseline design for an international neutrino factory [5]. Critical to the successful demonstration of EMMA [6] is the operation of its complex injection and extraction systems, whose design is summarised in [7] and in practice in this paper.

### INJECTION LINE

The ALICE (Accelerators and Lasers In Combined Experiments) to EMMA injection line, shown in Fig. 1, consists of a dogleg to extract the beam from the ALICE accelerator, a tomography section and finally a short dispersive section consisting of two dipoles, prior to the injection septum. The tomography section consists of a matching region which includes four quadrupoles followed by the diagnostic itself. The purpose of this section is to provide a quick and precise measurement of the Twiss parameters, emittance and transverse profiles. This also creates a fixed point in the line after which, if the tomography section is matched correctly, the Twiss parameters at all energies should be the same. This is useful because of the requirement to inject at a range of energies, which gives rise to different Twiss parameters

depending on the amount of RF focussing from the ALICE linac cavities (a function of their gradient) and how far off-crest they are (a function of their relative phase). The rest of the line after the tomography section can be used to optimise the energy dependent injection parameters into the ring.

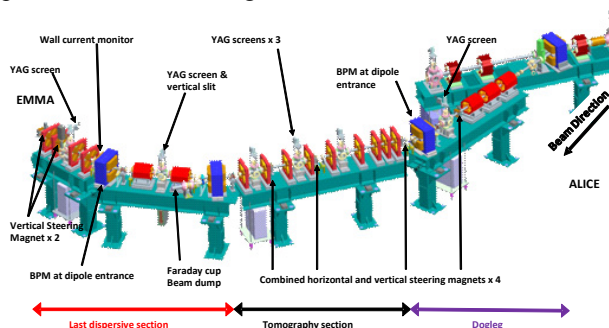


Figure 1: ALICE to EMMA injection line.

In order to improve the study of the physics of ns-FFAGs, it is important to minimise the energy spread of the beam at the start of the injection line. By carefully choosing the phases of the ALICE linac cavities, it has been possible to achieve an energy spread less than 0.05% (<7 keV at 15 MeV). The energy spread from the injector is minimised by adjusting the booster linac phase while monitoring the beam size on a YAG screen in a high dispersion region. The beam size is given by  $\sigma = \sqrt{\sigma_\beta^2 + (\eta\delta)^2}$ , where  $\sigma_\beta$  is the beam size in the absence of dispersion,  $\eta$  is the dispersion and  $\delta$  the energy spread. Thus in a high dispersion region, this is dominated by the contribution from the energy spread.

The energy spread at a YAG screen in the injection line is then minimised by varying the RF phases of the two main linac cavities around the combination of gradient and off-crest angles that give the correct energy. The design beta functions and dispersion in the EMMA injection line is shown in Figs. 2 and 3, respectively, together with the YAG screen used highlighted in green.

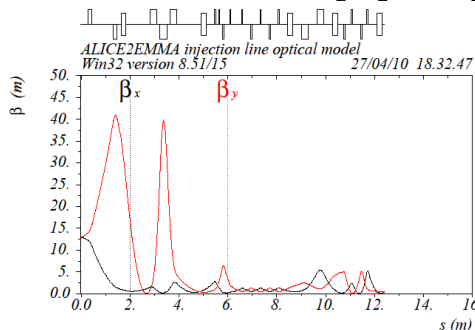


Figure 2: EMMA injection line layout and beta functions.

\*Work supported by the RCUK Basic Technology programme

<sup>#</sup>bruno.muratori@stfc.ac.uk

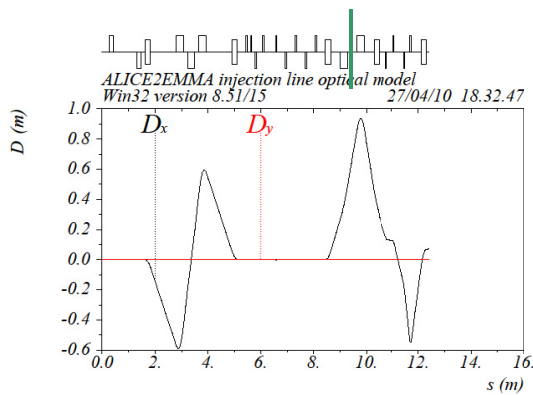


Figure 3: Dispersion in the EMMA injection line, with the YAG screen used highlighted in green.

A sample of the images recorded on the YAG is shown in Fig. 4.

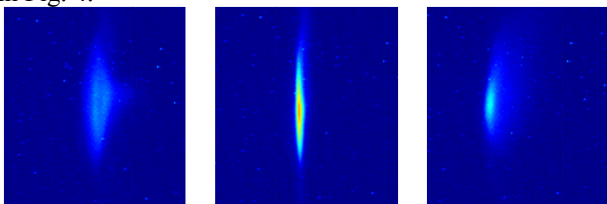


Figure 4: Variation of RF phase either side (left & right) of minimum energy spread (middle).

By plotting the beam size versus the RF phase, as shown in Fig. 5, we see that the minimum lies at around two degrees off-crest.

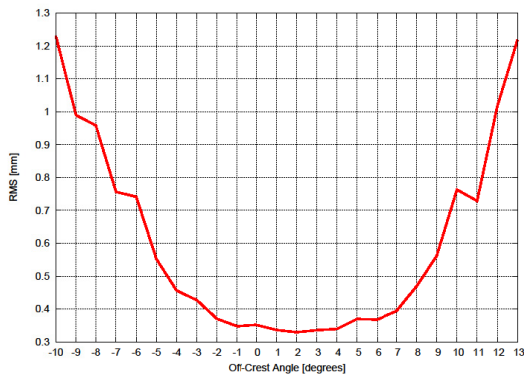


Figure 5: Beam size vs. off-crest angle.

So far the full optimisation for energy spread minimisation has only been done for 15 MeV and 20 pC. This has not yet been repeated at other energies, but the variation in uncorrelated energy spread with energy should be minimal as compared to the correlated energy spread that is controlled with the linac RF phase.

### EMMA RING

The basic elements of the injection system are a septum magnet and two kicker magnets, located in two successive long straight sections immediately after the long straight section where the septum is placed. The extraction system is simply a mirror image of the injection system. A tracking code FFEMMAG, developed S. Tzenov at

Daresbury Laboratory [8], was used to calculate all the injection parameters (septum strength and angle and kicker strengths). Other studies of injection and extraction into the EMMA ring [9, 10] using different codes give broadly similar results.

### PULSED MAGNETS COMMISSIONING

Commissioning and operation of the complicated injection and extraction pulsed-magnets scheme has proceeded well. The measured response of the magnets is in line with their design specifications. By reconstructing the injection orbit from the position and angle of the injected bunch after the exit of the septum, the magnet design can be checked. The required strength of the two kickers to take the beam on to the design orbit was then calculated and is shown in Fig. 6. The calculated kicker strength is not exactly the same as the measured values required for good injection, but are broadly similar, with the differences due to the specifics tuning of the lattice.

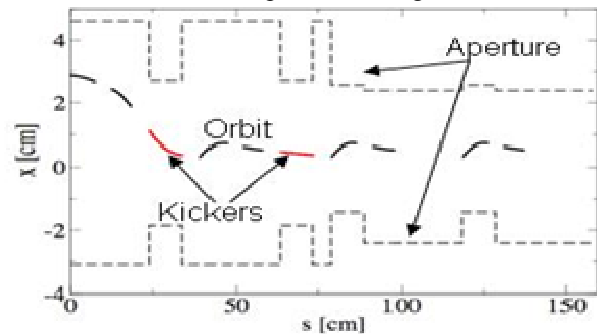


Figure 6: Injection region orbit, two normal cells (courtesy D. Kelliher).

### EXTRACTION LINE

The primary purpose of the EMMA extraction line is to make diagnostic measurements that cannot be made within the ring. Thus it is necessary for this line to be able to transport any energy from 10 (the minimum injection energy) to 20 MeV (the maximum design energy), with the beam coming from anywhere within the full acceptance of the EMMA ring.

It consists of an extraction septum, with the induced dispersion closed by several quadrupole magnets, followed by a dipole forming an irregular dogleg arrangement, as shown in Fig. 7.

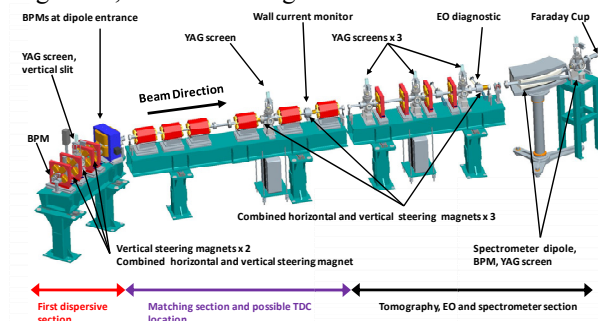


Figure 7: EMMA extraction line.

As part of this dogleg there is a YAG screen, which together with another screen in the following post-dipole dispersion-free straight, is used to measure the energy.

In the straight following the dogleg there are quadrupole magnets to match the beam either directly into a tomography section or into a proposed future transverse deflecting cavity. The tomography section is identical to that in the injection line, thus allowing the effect EMMA has on the projected transverse emittance and the transverse profiles to be determined accurately.

Between the tomography section and the spectrometer dipole, there is an Electro-Optic (EO) diagnostic to measure the bunch length and longitudinal profile [11]. After the spectrometer dipole there is also a Faraday cup for charge measurements.

Knowing that the revolution time is roughly 55.3 ns, it is possible to extract after an arbitrary number of turns by changing the strength of the two extraction kickers in coordinated steps, as shown in Fig. 8. The extraction septum has a pulse length much greater than the revolution time of the ring, and so does not need to be carefully set.

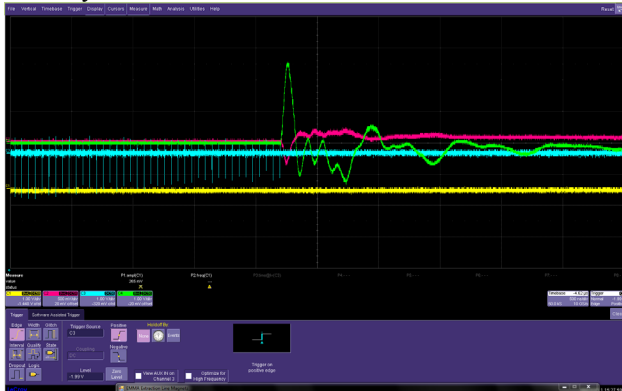


Figure 8: Scope display: first injection kicker (yellow), both extraction kickers (magenta and green) and the BPM signal from successive passes of the beam (cyan).

The action of the injection kicker is too early and cannot be seen in Fig. 8, whereas the effect of the extraction kickers is evident.

The first complete extraction, together with consistent extracted energy measurements, took place on the 17<sup>th</sup> April 2011. The images recorded in Fig. 9 are taken on the first and fourth YAG screens in the extraction line - both with RF (septum: 5.7 V, dipole: 4.238 A) and without RF (septum: 8.881 V, dipole: 7.13 A). These show that EMMA accelerated the injected beam by a factor of 1.68 from a momentum of 12.5 ( $\pm$  0.1) MeV/c at injection to 21 ( $\pm$  1) MeV/c at extraction. The dipole field was used in this calculation as it gave a more consistent measurement of beam energy than the septum field, due to the variation in trajectory inside the septum, which varies strongly with ring energy.

## CONCLUSION

The successful commissioning of EMMA, the world's first ns-FFAG accelerator, would have been impossible

without its complex injection and extraction schemes also performing well. Progress with the analysis of tomographic data from the injection line is underway [12] and measurement of the beam energy in the extraction line has been critical in demonstrating that acceleration of the injected beam has been achieved, Fig 9 and [13].

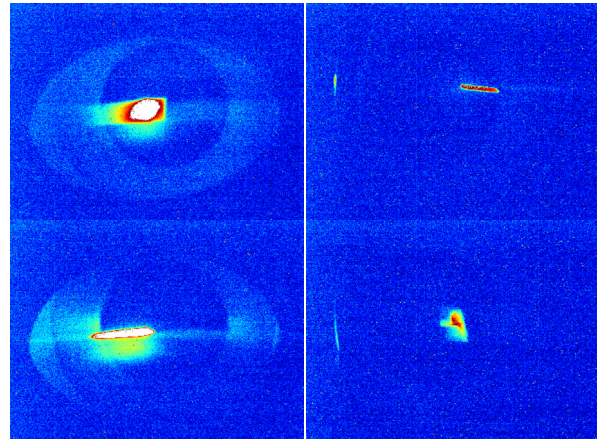


Figure 9: Extraction on the first YAG screen (L), the fourth (R); with RF (top), without RF (below).

## REFERENCES

- [1] S. L. Smith, "EMMA, the World's First Non-Scaling FFAG Accelerator", Proc. PAC09, Vancouver, (2009).
- [2] R. Edgecock, Proc. IPAC10, Kyoto, Japan, (2010).
- [3] K. Peach et al, "PAMELA Overview: Design Goals and Principles", Proc. of PAC09, Vancouver, (2009).
- [4] C. Bungau, R. J. Barlow, R. Cywinski, "Reactor Design Studies for an Accelerator Driven System", Proc. of PAC09, Vancouver, BC, Canada (2009).
- [5] K. Long (Ed), "An International Scoping Study of a Neutrino Factory and Super-beam Facility", CARE-Report-2005-024-BENE, (2005).
- [6] J. S. Berg, "The EMMA Main Ring Lattice". CONFORM report. (2008).
- [7] B.D. Muratori et al., 'Injection and Extraction for the EMMA NS-FFAG', Proc. EPAC08, Genoa (2008).
- [8] J. K. Jones, B. D. Muratori, S. L. Smith and S. I. Tzenov, "Dynamics of Particles in Non-Scaling FFAG Accelerators". Progress in Physics, Vol. 1 72-82 (2010).
- [9] J. S. Berg, "An Injection/Extraction Scenario for EMMA", Proc. PAC09, Vancouver, Canada (2009).
- [10] Y. Giboudot, D. Kelliher, F. Méot and T. Yokoi, "Beam Dynamics Simulations Regarding the Experimental FFAG EMMA, Using the On-line Code". Proc. IPAC2010, Kyoto, Japan (2010).
- [11] G. Berden et al, Proc. EPAC04, Lucerne, Switzerland (2004).
- [12] TUPC149 and TUPC150, these proceedings.
- [13] S. Machida et al. (2011), 'Acceleration in the linear non-scaling fixed field alternating gradient accelerator EMMA, Electron Model for Many Applications' - to be published.